Published in final edited form as:
Biomaterials. 2012 May ; 33(15): 3783–3791. doi:10.1016/j.biomaterials.2012.02.027.

Mussel-Inspired Silver-Releasing Antibacterial Hydrogels

Dominic E. Fullenkamp[#,1,2], **José G. Rivera**[#,1,2], **Yong-kuan Gong**[3], **K. H. Aaron Lau**[1,2], **Lihong He**[1,2], **Rahul Varshney**[1,2,4], and **Phillip B. Messersmith**[*,1,2,4,5,6,7]

[1]Biomedical Engineering Department, Northwestern University, Evanston, IL, 60208, USA

[2]Chemistry of Life Processes Institute, Northwestern University, Evanston, IL, 60208, USA

[3]Key Laboratory of Synthetic and Natural Functional Molecule Chemistry (Ministry of Education), College of Chemistry and Materials Science Northwest University, 229 Taibai Beilu, Xi'an 710069, P. R. China

[4]Chemical and Biological Engineering Department, Northwestern University, Evanston, IL, 60208, USA

[5]Materials Science and Engineering Department, Northwestern University, Evanston, IL, 60208, USA

[6]Institute for Bionanotechnology in Medicine, Northwestern University, Evanston, IL, 60208, USA

[7]Robert H. Lurie Comprehensive Cancer Center, Northwestern University, Evanston, IL, 60208, USA

Abstract

A silver-releasing antibacterial hydrogel was developed that simultaneously allowed for silver nanoparticle formation and gel curing. Water-soluble polyethylene glycol (PEG) polymers were synthesized that contain reactive catechol moieties, inspired by mussel adhesive proteins, where the catechol containing amino acid 3,4-dihydroxyphenylalanine (DOPA) plays an important role in the ability of the mussel to adhere to almost any surface in an aqueous environment. We utilized silver nitrate to oxidize polymer catechols, leading to covalent cross-linking and hydrogel formation with simultaneous reduction of Ag(I). Silver release was sustained for periods of at least two weeks in PBS solution. Hydrogels were found to inhibit bacterial growth, consistent with the well-known antibacterial properties of silver, while not significantly affecting mammalian cell viability. In addition, thin hydrogel films were found to resist bacterial and mammalian cell attachment, consistent with the antifouling properties of PEG. We believe these materials have a strong potential for antibacterial biomaterial coatings and tissue adhesives, due to the material-independent adhesive properties of catechols.

1. Introduction

The mussel byssus has been a source of biomaterials inspiration due to its water-resistant, material-independent adhesive abilities.[1–4] Mussels secrete a protein-rich liquid from the

Phillip B. Messersmith, Biomedical Engineering Department, Northwestern University, 2145 Sheridan Road, Evanston, IL 60208, Phone (847) 467-5273, Fax (847) 491-4928, philm@northwestern.edu.
[#]Both authors contributed equally to this work

phenol gland in the mussel foot to form an adhesive holdfast.[5] 3,4-Dihydroxy-L-phenylalanine (DOPA) makes up a significant fraction of the amino acid residues in protein extracted from the *Mytilus edulis* phenol gland and is thought to be a key component of the mussel's adhesive strategy.[4–7] _ENREF_2 The catechol side chain of DOPA readily oxidizes to form reactive species that can further undergo Michael-type addition or Schiff base formation with nucleophiles, and radical coupling with other catechols.[5] Such reactions are initiated upon DOPA oxidation and are thought to be the basis of rapid solidification of the secreted protein liquid into a hardened adhesive. Additional adhesive mechanisms of catechols include coordination bonds with a diversity of metals and inorganic surfaces, hydrogen bond formation, and π-π aromatic interactions. Our group and others have focused on $NaIO_4$, enzymatic, or metal-coupled oxidation of catechol-functionalized polymers for the purposes of adhesion to material and tissue surfaces. [2, 3, 8–11]

Hydrogels are water-swollen polymer networks of interest to the biomaterials community for potential use in a diverse range of applications including structural biomaterials, surface coatings, and sensing applications.[12, 13] Biomaterials with inherent antibacterial properties are useful for the prevention of infections associated with surgical interventions and for preventing medical device-related biofilm formation. Recently, interest has grown in the development of biomedically relevant materials containing silver, due to its well-known bactericidal properties. Silver nitrate solutions have historically been used for the prevention of gonococcal eye infections in the newborn, and various preparation of silver or silver salts have been used in the treatment of burns and wound dressings.[14–17] The silver ion, Ag(I), is believed to be the active antimicrobial agent, possessing antibacterial activity at low concentrations (10^{-9} – 10^{-6} M).[16–19] The use of silver as an antimicrobial agent has received increasing attention due to the surge of antibiotic-resistant bacterial strains that have become a major public health concern.[16, 20] Silver impregnated biomaterials have been investigated, and several commercial products are currently available.[16, 19, 21, 22] Silver alloy impregnated urinary catheters have been shown to reduce the risk of bacteriuria. [23]

Various approaches have been previously reported for the preparation of silver-hydrogel composites. Varaprasad et al. reported a method for embedding colloidal silver into hydrogels, via reduction of silver nitrate by sodium borohydride during polymer gelation. [24] Zan and coworkers prepared silver-containing hydrogels via simultaneous photolysis-initiated reduction of silver nitrate and polymerization/cross-linking of bifunctional monomers.[25] Structural control in the formation of silver nanoparticles was also achieved by the reduction of silver nitrate inside a pre-formed hydrogel network.[26]

Recent work from our lab has demonstrated redox coupling between DOPA-modified polymers and Au(III) or Ag(I) metal ions, leading to formation of noble metal nanoparticle cores surrounded by a polymerized shell of catechol polymer cross-linked via catechol oxidation.[27] These findings led us to speculate that similar redox reactions could be exploited to form covalent polymer hydrogels via Ag(I) reduction coupled to catechol oxidation, leading to in-situ formation of Ag nanoparticle-filled gels. Interestingly, while literature reports exist for the use of Ag(I) as an oxidizing agent for catechols,[28, 29] to our knowledge, no reports exist that utilize Ag(I) to promote catechol oxidation for polymer hydrogel cross-linking.

Herein, we describe the preparation of antibacterial hydrogels by taking advantage of spontaneous redox reactions between a branched catechol-derivatized poly(ethylene glycol) (cPEG, Figure 1) and Ag(I). The strategy employs silver both to induce hydrogel cross-linking via catechol oxidation (Figure 1) and as a precursor for Ag nanoparticle formation,

imparting antibacterial activity to the formed hydrogel. Model studies were performed to correlate Ag(I) reduction and catechol oxidation to Ag nanoparticle formation and polymer cross-linking, and the formation of antibacterial silver-containing bulk hydrogels and coatings is illustrated.

2. Materials and Methods

2.1. Materials

4-arm PEG amine (MW~10,000 g/mol) and mPEG amine (MW~ 5,000 g/mol) were obtained from Laysan Bio Inc. (Arab, AL). 3-(3,4-dihydroxyphenyl) propionic acid (DHPA, 98 %) was purchased from Alfa Aesar (Ward Hill, MA). Silver nitrate (99.8 %) and triethylamine (99 %) were acquired from Sigma-Aldrich (Milwaukee, WI). N-hydroxybenzotriazole (HOBt) from Advanced ChemTech (Louisville, KY) and O-benzotriazole-N,N,N',N'-tetramethyl-uronium-hexafluoro-phosphate (HBTU) from EMD Biosciences (La Jolla, CA) were used without further purification. Tris(hydroxymethyl)aminomethane (Tris) was obtained from Fisher Scientific (Fair Lawn, NJ). Phosphate buffered saline (PBS) was prepared by dissolving 8.00 g NaCl, 0.20 g KCl, 1.15 g Na_2HPO_4, and 0.24 g KH_2PO_4 into ~900 mL of water. The pH was adjusted to 7.40 with 1 M NaOH or 1 M HCl, and the solution was mixed with additional water to 1.00 L in a volumetric flask. Bacteria strains *Staphylococcus epidermidis* RP62A (ATCC 12228), and *Pseudomonas aeruginosa* (ATCC 27853) were purchased from American Type Culture Collection (Manassas, VA). Tryptic soy agar, tryptic soy broth and tetracycline disks for zone of inhibition assays were obtained from Becton, Dickinson and Co. (Franklin Lakes, NJ). Silicon wafers (University Wafer, Boston, MA) were coated with 12–14 nm of TiO_2 by physical vapor deposition using electron beam evaporation (Edwards Auto500; 10^{-5} Torr with a TiO_2 target). Prior to use, all substrates were sonicated successively for 10 min in 2-propanol and MQ water, dried in a stream of N_2, and cleaned by exposing to O_2 plasma (Harrick Scientific, Ossining, NY) for 3 min.

2.2. cPEG and mPEG-Cat synthesis and characterization

cPEG and mPEG-Cat was synthesized as has been previously reported.[30] cPEG charaterization: MALDI-TOF MS M_n ~10,900–11,400 (depending on batch); ^{1}H NMR ($CDCl_3$) δ (ppm): 6.5–7.0 (m, 3H, aromatic), 2.85 (s, 2H, -NHCO-CH_2-), 2.5 (s, 2H, CH_2, adjacent to aromatic), 3.51–3.67 (m, -O-CH_2CH_2-). mPEG-Cat charaterization: MALDI-TOF MS M_n ~5,600; ^{1}H NMR ($CDCl_3$) δ (ppm): 6.5–7.0 (m, 3H, aromatic), 2.85 (s, 2H, adjacent to aromatic), 2.5 (s, 2H, -NHCO-CH_2-), 3.51–3.67 (m, -O-CH_2CH_2-), 3.35 (s, 3H, OCH_3).

2.3. Hydrogel formation: bulk hydrogels

All solutions for gel formation were made using Tris buffer (100 mM, pH 8.5). To prevent AgCl precipitation, Tris buffer was prepared from Tris base and brought to pH 8.5 with 1 M nitric acid. The final concentration of cPEG was kept constant (150 mg/mL, ~13.2 mM – depending on the molecular weight of the batch), and the concentration of $AgNO_3$ was varied according to the desired Ag:catechol molar ratio. A typical procedure for gel formation consisted of mixing equal volumes of cPEG (300 mg/mL, ~26.4 mM polymer, ~106 mM endgroup) and $AgNO_3$ (212 mM). This produced a 2:1 Ag:catechol gel. A color change from (orange/brown) to (dark green/black) was observed 20 s after mixing. We refer to these materials as Ag-cPEG gels throughout this manuscript. Gelation times, as reported in Table 1, were determined by the inversion technique.

2.4. Hydrogel formation: hydrogel coatings

Ag-cPEG coatings were formed by spin-coating from a precursor solution containing cPEG (5 mg/mL) and $AgNO_3$. The precursor was freshly mixed immediately before use and contained two equivalents of Ag(I) per catechol. The cPEG/$AgNO_3$ solution did not immediately form a hydrogel, which permitted spin-coating onto clean TiO_2 coated Si wafer at a speed of 4000 rpm (Chemat Technology Spin-Coater, Northridge, California, USA). After heating at 100 °C for 30–60 min, the Ag-cPEG coated TiO_2 substrates were stored at room temperature until use.

2.5. Ellipsometry

A M-2000 spectroscopic ellipsometer (J.A. Woollam, Lincoln, Nebraska, USA) was used to measure Ag-cPEG coating thickness on TiO_2-coated silicon wafers. Measurements were made at wavelengths from 370–1000 nm. The spectra were fitted with a multilayer model in the WVASE32 software (J.A. Woollam Lincoln, Nebraska, USA). Optical properties of the bare substrate were fitted using a standard Si or TiO_2 model, while properties of the polymer layer were fitted using a Cauchy model. The average thickness of six samples was obtained, representing the “dry” thickness of the polymer under ambient conditions.

2.6. Oscillatory rheometry

Rheometry was performed on an Anton Paar MCR 300 rheometer at 20 °C in a Peltier hood with an evaporation blocker and a CP 25-2 cone and plate fixture (25 mm diameter, 2° cone angle). cPEG and silver solutions were mixed and immediately pipetted onto the rheometer baseplate before gel formation. The fixture was brought down into contact with the gel precursor liquid within 2 min of mixing. Time tests were performed at 5 % strain and 10 rad/s. Frequency sweeps were performed at 5 % strain from 100 rad/s to 0.1 rad/s. Strain sweeps were performed at 10 rad/s from 1 to 1000 % strain.

2.7. Model gel permeation chromatography (GPC) studies of gel formation using mPEG-Cat

The reaction between mPEG-Cat (M_n ~5,600 Da by MALDI-TOF-MS) and Ag(I) was performed at 60 mM endgroup concentration to closely replicate gel formation conditions. Polymers and $AgNO_3$ solutions were prepared with Tris buffer (100 mM, pH 8.5, pH adjusted with 1 M nitric acid). 3.0 mg aliquots of mPEG-Cat, prepared using a speedvac, were dissolved into 4.87 μL buffer. 4.87 μL of 120, 240, and 480 mM $AgNO_3$ solutions were added to the mPEG-Cat solutions to make 1×, 2×, and 4× Ag(I). For the 0× Ag(I) solution an additional 4.87 μL of buffer was added. After 1 h, the reactions were quenched by adding 290 μL 0.10 M EDTA to bind any unreacted Ag(I) and bring the polymer concentration to 10 mg/mL. Samples were then centrifuged to remove silver particles and the supernatant was syringe filtered using 0.2 μm PTFE filters. GPC was performed with a mobile phase of 50 mM citrate, 100 mM $NaSO_4$, pH 3.5. Each sample (10 μL) was injected into an Agilent 1100 Series HPLC (flow rate 1.0 mL/min) equipped with a Shodex KW-803 GPC column (heated to 40 °C) and in line with Wyatt Dawn Heleos II and Optilab T-rEx dRI detectors. PEG standards (Varian) of 3,930, 7,920, and 12,140 kDa were prepared in GPC buffer at 10 mg/mL for each polymer. A control sample of mPEG-Cat was dissolved at 10 mg/mL in the GPC buffer. Wyatt Astra software was used to calculate M_n, M_w, and the relative percentages of monomer vs multimer of mPEG-Cat. The PEG dn/dc was taken to be 0.136 mL/g.

2.7. UV-Vis spectroscopy

UV-Vis spectroscopy was performed on an HP8452 PDA spectrometer using Plastibrand 1.5 mL disposable cuvettes. Final solution concentrations were a 100× dilution of Ag-cPEG gels

at 2:1 Ag:catechol. cPEG and $AgNO_3$ solutions were freshly prepared before use. 400 μL of 5 mM Tris buffer (pH 8.5) was added to 876 μL water and the sample was blanked. 300 μL of a 10 mg/mL cPEG solution in water was added and pipetted several times, followed by addition of 424 μL of a 5 mM $AgNO_3$ solution in water. The final solution was pipetted several times until it was well mixed. The first spectrum was acquired 30 s after silver addition and once every 3 min thereafter until 27 min. After 30 min elapsed time, samples were diluted 10× into water because of high absorbance near the Ag nanoparticle plasmon band maximum.

2.8. TEM

Transmission electron microscopy (TEM) was performed on a Hitachi HD-2300 ultra high resolution FE-STEM (Hitachi High Technologies, Inc.). 5 μL of the diluted reactions (previously used for UV-Vis experiments) were dropped on EM grids (Ted Pella) and allowed to dry before analysis.

2.9. Ag-cPEG gel swelling experiments

Once the silver nitrate and cPEG solutions were completely mixed (~1 min), 100 μL of the resultant mixtures were transferred into cylindrical molds (9 mm in diameter, 2 mm tall) and covered with a glass slide on each side. After 1 day, the gels were taken out of the molds, weighed, and immersed in 5 mL of PBS for 7 days. The gels were then taken out of the PBS solution and re-weighed in order to calculate the change in weight. Gel swelling % was calculated with the formula: $[(W_2 - W_1)/W_1] \times 100$ %, where W_1 and W_2 are the masses of the hydrogels before and after being swollen in PBS respectively.

2.10. Determination of silver release by ICP-MS

Silver release from gels was analyzed by Inductively Coupled Plasma – Mass Spectrometry (ICP-MS) using a Thermo XSeries II ICP-MS (Thermo-Fisher). Samples were prepared by immersing the above described Ag-cPEG gels disks (Ag:catechol mol ratio = 2.0) in 5 mL of PBS for 14 days at ambient temperature. The PBS was replaced after 1, 2, 3, 4, 5, 6, 8, 10, 12, and 14 days and analyzed for silver content. For ICP-MS analysis, an aliquot of the PBS solution (500 μL) was diluted with 4.4 mL of ultra-pure water (18 MΩ-cm) and 25 μL of an internal standard mixture of Sc, Tb, Y, In, and Bi (CPI International). Standards between 0 and 500 ppb were made using a 1000 ppm standard Ag(I) solution (CPI International). Silver standards and samples were prepared and analyzed in a matrix of 2 % nitric acid.

2.11. Bacterial growth inhibition assay

The Ag-cPEG gel growth inhibition against *S. epidermidis* and *P. aeruginosa* was evaluated. 5.0 mL of a 1×10^8 colony forming units (CFU) culture of either bacterial strain in tryptic soy broth (TSB) was mixed with 100 mL of TSB agar at 45 °C. 25 mL of the resultant mixture was transferred to 150 mm diameter petri dishes. After solidification of the agar (~3 min), Ag-cPEG gel disks were placed on top of agar plates and placed in an incubator at 37 °C for 36 hours. Zones of bacterial growth inhibition were measured and compared to cPEG hydrogels cross-linked with sodium periodate and tetracycline antibiotic disks (30 μg). Periodate gels were formed by a previously reported procedure[2] and leached of their oxidation byproducts by incubation in 5 mL of water for 1 week, with an exchange of the water at day 3.

2.12. Bacterial cell attachment assay

12 mm by 12 mm substrates were sterilized in 70 % ethanol solution and UV irradiation of the test surface for 30 min. The surfaces were equilibrated with sterilized MQ water for 4 h followed by culture medium (PBS: tryptic soy broth = 1:1) for 1 h. *S. epidermidis* were

streaked from frozen glycerol stocks onto tryptic soy agar and incubated overnight at 37 °C. A few colonies were then used to inoculate 25 mL of sterile tryptic soy broth (TSB) and grown overnight at 37 °C. The bacterial suspension was then seeded on uncoated and Ag-cPEG coated TiO_2 at a concentration of 1–9 × 10^8 CFU in a 12-well cell culture plate. After incubation at 37 °C and under gentle rocking movement for 24 h, the surfaces were rinsed with PBS to remove loosely adhered bacteria. The attached bacteria were then stained with 2 μL/mL Syto 9 in PBS and visualized using a Leica epifluorescence microscope (40× magnification) equipped with a SPOT RT digital camera (Diagnostics Instruments, Sterling Heights, MI, USA). Three identical surfaces for each experiment were analyzed for statistical purposes, resulting in a total of 9 images per time point for each modification. The microscopy images were quantified using threshold analysis in Metamorph (Molecular Devices, Downingtown, PA, USA).

2.13. Mammalian cell viability assay

The viability of 3T3 Swiss albino mouse fibroblasts (CCL-92, ATCC, Manassas, VA) in response to the Ag-cPEG gel conditioned media was tested with the MTS (3-(4,5-dimethylthiazol-2-yl)-5-(3-carboxymethoxyphenyl)-2-(4-sulfophenyl)-2H-tetrazolium, inner salt) cell proliferation assay (CellTiter 96® AQueous, Promega, Madison, WI). Fibroblasts were first cultured at 37 °C with 5 % CO_2 in Dulbecco's modified Eagle media (DMEM) containing 10 % calf bovine serum (CBS) and 100 U/mL of penicillin/streptomycin. They were harvested using 0.25 % trypsin-EDTA, counted using a hemacytometer immediately before use, and re-suspended in the cell-culture media at a concentration of 1×10^5 cells/mL. Test cell culture media was prepared by incubating cross-linked Ag-cPEG hydrogel disks (5 mm in diameter, 2 mm tall, cross-linked overnight) in the cell culture media for 1 d at 4 °C (500 μL to a disk, each in wells of 24-well plates, sealed with cover adhesive). Control media without gel material was concurrently aged in parallel wells. After aging, the test and control media were mixed at varying ratios in wells of 96-well plates to a total volume of 50 μL per well. 50 μL of suspended 3T3 fibroblasts (50 μL) was mixed into each well and the plates were incubated at cell culture conditions. At the prescribed experimental time point (24 h and 48 h), 20 μL of premixed MTS solutions was mixed to each well and the plates were further incubated at cell culture conditions for 4 h. During this time MTS was bioreduced by live-cells into a formazan product that is soluble in tissue culture medium. After incubation, the optical absorption of the formazan at 490 nm was read by a multiplate reader (Synergy 2, BioTek, Winooski, VT) and used as a proxy of cell viability. The average baseline absorbance measured for control media without cells (negative control) was subtracted from all results to obtain the sample absorbances, which were then normalized by the values measured for control media seeded with cells (positive control). All experiments were performed in triplicate.

2.14. Mammalian cell attachment assay

3T3-Swiss albino fibroblasts were maintained at 37 °C and 5 % CO_2 in Dulbecco's modified Eagle's medium (DMEM) containing 10 % fetal bovine serum (FBS) and 100 U/mL of penicillin/streptomycin. Immediately before use, fibroblasts of passage 12–16 were harvested using 0.25 % trypsin-EDTA, resuspended in DMEM with 10 % FBS and counted using a hemacytometer. Modified and unmodified TiO_2 substrates were placed in a 12-well tissue-culture polystyrene plate and sterilized by exposure to UV light for 30 min. After the substrates were in contact with 1 mL of PBS for 1 h at 37 °C, the buffer solution was aspirated and 1 mL of DMEM containing FBS was added to each well. After incubation for 30 min at 37 °C and 5 % CO_2, fibroblast cells were seeded on each substrate at a density of 4.2×10^3 cells/cm^2. The surfaces were maintained in DMEM with FBS at 37 °C and 5 % CO_2 for 4, 24, 72 and 168 h. Subsequently, the medium was aspirated from each well to remove any non-adherent cells and PBS was used to rinse the substrates and wells.

Fibroblasts were stained with 2.5 mM calcein-AM in complete PBS for 50 min at 37 °C, and transferred to new culture plates with PBS buffer for epifluorescent microscope counting. For the 7-day adhesion experiments, the surfaces were reseeded with 3T3 fibroblasts at a density of 4.2×10^3 cells/cm^2 on the third day after changing the media. Quantitative cell-attachment data was obtained by acquiring three images from random locations on each surface using a Leica epifluorescence microscope (W. Nuhsbaum Inc., McHenry, IL, USA) equipped with a SPOT RT digital camera (Diagnostics Instruments, Sterling Heights, MI, USA). Three identical surfaces for each experiment were analyzed for statistical purposes, resulting in a total of 9 images per time point for each modification. The microscopy images were quantified using threshold analysis in Metamorph (Molecular Devices, Downingtown, PA, USA).

3. Results

In this work, we investigated $AgNO_3$-mediated oxidation of catechol functionalized 4-arm-PEG (cPEG, Figure 1), hypothesizing that catechol oxidation coupled with Ag(I) reduction would result in spontaneous formation of silver nanoparticle embedded hydrogels, which would have inherent silver-based antibacterial properties. We believe that these materials may be useful as antibacterial tissue adhesives or biomaterial coatings.

3.1 Hydrogel formation and characterization

Ag-cPEG hydrogels were formed by the addition of silver nitrate to cPEG at basic pH (pH = 8.5), resulting in a color change from orange/brown to dark green/black within one minute, followed by gradual gelation. As seen in Table 1, the mol ratio of Ag:catechol strongly affected the rate of gelation and gel swelling. Gelation times ranged from 1 h (molar ratio = 0.5) to 10 min (mol ratio = 4.0). We also noticed increased rigidity in gels as the Ag:catechol ratio was increased. Gels formed using a Ag:catechol ratio of 0.5 and 1.0 were very fragile and could not be removed from the vials without fracturing. Increasing the Ag:catechol ratio to 2.0 and greater resulted in qualitatively more rigid gels. Figure 2 shows photographs of a freestanding Ag-cPEG gel formed at a Ag:catechol ratio of 2.0. This gel was easy to handle and formed within a reasonable period of time (~20 min), which is why we chose this stoichiometry for the remainder of our experiments.

The mechanical properties of these gels were studied by oscillatory rheometry. Figure 3a shows the time-dependent maturation of a Ag-cPEG gel at a 2:1 Ag:catechol ratio. Although initial time points indicated elastic properties ($G' > G''$), qualitative observations by vial inversion showed gelation times to be on the order of 20 min. Within 100 min, the storage modulus of the gel appears to plateau. The frequency sweep (Figure 3b) is consistent with a covalently cross-linked hydrogel with $G' >> G''$ at all measured frequencies. The strain sweep (Figure 3c) showed a yield strain of ~200 % strain.

Thin adherent hydrogel coatings of Ag-cPEG were easily formed on TiO_2 substrates by spin-coating prior to gelation. In this case, the Ag:catechol ratio was maintained at 2.0 although the cPEG concentration was reduced to 5 mg/mL to allow for spin-coating from a liquid precursor solution. Thermal annealing at 100 °C for 1 h resulted in 25 nm thick Ag-cPEG coatings (dry) as determined by ellipsometry. XPS analysis (Figure S1) indicated only the presence of C, O and Ag in the coating, confirming that the coating thickness was greater than 10 nm.

3.2 GPC characterization of mPEG-Cat reaction with Ag(I)

mPEG-Cat (Figure 1) was used as a model monofunctional polymer to characterize the reaction of Ag(I) and catechol-modified polymers. The 60 mM polymer concentration used

was chosen to parallel the ~60 mM catechol endgroup concentration of the gels. Figure 4 shows GPC chromatograms after 1 h of mPEG-Cat and Ag(I) reactions. As seen in the figure, increasing the Ag(I) to mPEG-Cat ratio increases the amount of dimer and multimer formed. The relative amount of dimer and multimer to monomer was calculated using light scattering data acquired in series with the dRI measurement through the Wyatt Astra software. For 0×, 1×, 2×, and 4× Ag(I)/mPEG-Cat it was determined that 3%, 9%, 21%, and 33% of the polymer was in the form of dimer or multimer, respectively, with the remaining polymer being the monomer form. Polymer molecular weights calculated by the Astra software were consistent with the expected molecular weights, e.g., for the 2× Ag(I)/mPEG-Cat reaction, the monomer and dimer/multimer M_n was found to be 6.25 and 15.2 kDa, respectively (the dimer and multimer peaks cannot be cleanly separated). In a control experiment where mPEG-Cat was dissolved in the GPC buffer only (at pH 3.5 in the absence of an oxidizing agent, catechols are expected to be stable towards oxidation and cross-linking), 1% of the polymer was found to be in the dimer or multimer form.

3.2. Dilute solution nanoparticle characterization

UV-Vis spectroscopy was used to further study silver nanoparticle formation as a consequence of the redox reaction of Ag(I) with cPEG. A 100× dilution of the 2:1 Ag:catechol Ag-cPEG gel solution was used in order to keep absorbance measurements within instrumental limits. This low polymer concentration was insufficient to induce gel formation. Polymer, silver, and buffer concentrations were scaled proportionally. As shown in Figure 5a, a plasmon band with a maximum absorbance at 430 nm developed, which is consistent with silver nanoparticle formation.[27] Figure 5b shows the solution from Figure 5a diluted 10× after 30 min and 2 days. It can be seen that the reaction continues slowly even after 30 min, and a weak peak develops around 560 nm by 2 days, possibly due to quinone tanning. While UV-Vis would generally be a good technique to identify the reactive quinone intermediate, the plasmon peak is expected to have significant overlap with the quinone peak (~400 nm),[31] making it difficult to detect. Ag nanoparticle shape and size distribution were evaluated by TEM. Figure 6 shows images of nanoparticles obtained from the UV-Vis study shown in Figure 5, of a 2:1 Ag:catechol reaction with cPEG. The nanoparticles are mostly round-shaped and well-dispersed, with diameters up to ~50 nm.

3.3. Silver release properties of bulk gels

Silver release from the Ag-cPEG gels was evaluated by ICP-MS. The gels were immersed in excess PBS for up to two weeks with periodic sampling of the Ag concentration in the PBS solution. Figure 7 shows the cumulative release of silver from the Ag-cPEG hydrogels during the first two weeks. The total amount of silver that was released from the hydrogels during the first two weeks was ~10 μg, corresponding to ~1 % of the total amount of silver inside the hydrogel disks. The release kinetics up until at least the two week time point are roughly zero order, which is important for many applications when a sustained release of silver is desired.

3.4. Bacterial viability and attachment

The antibacterial activity of the gels was investigated by measuring their ability to inhibit *S. epidermidis* and *P. aeruginosa* growth on agar culture plates. After 36 h of incubation, bacterial colonies were clearly observed in contact with control gels, while there were no bacterial colonies found in contact with the Ag-cPEG hydrogels. The Ag-loaded gels also exhibited a surrounding ‘zone of inhibition’ (ZOI) to bacterial growth (145–155 % of the original gel size), which was similar to the ZOI shown by tetracycline loaded disks (Table 2).

Hydrogel coatings formed by spin-coating a cPEG/$AgNO_3$ precursor solution onto TiO_2 were evaluated for their ability to resist bacterial cell attachment. As can be seen in Figure 8, unmodified TiO_2 supported rapid and extensive attachment of *S. epidermidis* within the first 24 h, however attachment onto Ag-cPEG coated TiO_2 was reduced by >99.9 % compared to unmodified TiO_2 over the same time period.

3.5 Mammalian cell viability and attachment

To further assess the utility of these hydrogels as biomaterials, we studied the effect of the eluent from the Ag-cPEG hydrogels on 3T3 fibroblasts using the MTS assay. Gels were incubated in growth media overnight and then this conditioned media was diluted with fresh media to a final composition of 0–100 %. Following standard MTS protocol, it was then mixed with an equal volume of fibroblast suspension and cell viability was assessed at 24 and 48 h. Using this procedure, a maximum of 50 % Ag-cPEG gel eluent was able to be studied. Shown in Figure 9 is the effect of the aged media on cell viability. As can be seen, at both time points and all dilutions of the aged media, fibroblast viability was not greatly affected.

The Ag-cPEG hydrogel coatings were also resistant to mammalian cell attachment, as shown in Figure 10. In this experiment, 3T3 cells were cultured on Ag-cPEG coated TiO_2 for up to 7 days and cell adhesion measured by fluorescence microscopy and image analysis. The results reveal that the Ag-cPEG coatings are highly resistant to mammalian cell attachment over a several day period as indicated by a dramatic decrease in 3T3 cell attachment compared to unmodified TiO_2.

4. Discussion

In this work, we hypothesized that we could take advantage of the ability of Ag(I) to oxidize catechol-functionalized polymers to simultaneously induce covalent gel formation and silver nanoparticle formation, further hypothesizing that these materials would possess antibacterial properties through the slow release of Ag(I). The mechanism of gel formation is supported through several lines of evidence. As shown in Table 1, the speed of gel formation and the degree of cross-linking (as evidenced by decreased swelling) increase with increased Ag(I). Polymer covalent bond formation was conclusively demonstrated with model monofunctional mPEG-Cat polymers by GPC (Figure 4). Increasing the amount of Ag(I) increased the extent of the reaction. Although catechols are prone to spontaneous oxidation at basic pH, autooxidation was insufficient to form cPEG gels at basic pH without the addition of Ag(I) (Table 1). GPC studies of the reactions showed that auto-oxidation did not contribute significantly to covalent bond formation over 1 h (Figure 4, 0× Ag sample), with only 3% of the polymer in the 0× Ag(I) solution in the dimer or multimer form. Silver nanoparticle formation was observed in dilute cPEG-Ag(I) solutions (but otherwise identical to gel solutions, Figure 5 and Figure 6), demonstrating the reduction of Ag(I) to Ag(0) in the presence of cPEG. We therefore propose the overall reaction shown in Figure 1, involving reduction of Ag(I) to Ag(0) coupled with catechol oxidation and subsequent cross-linking of the quinone and catechol. Although the redox reaction shown in the reaction scheme results in the production of two protons per catechol, the buffering capacity was sufficient to prevent substantial reduction in pH.

Gel mechanical properties were consistent with a covalently cross-linked hydrogel. After curing it does not flow and can be picked up (Figure 2), with G' and G'' essentially frequency independent (Figure 3b). Rheological characterization (Figure 3) revealed a lower modulus and increased strain at yield in Ag-cPEG gels, when compared to $NaIO_4$ cross-linked cPEG gels.[2, 3] This is consistent with a decrease in the cross-linking density of the

Ag-cPEG gel relative to $NaIO_4$ gels, and therefore, it appears that the $NaIO_4$-based reaction more efficiently cross-links catechols.

Silver nanoparticle formation is consistent with earlier work from our group on the creation of silver nanoparticles via reduction of ionic silver by linear catechol end-modified polymers.[27] A stabilizing PEG shell on the nanoparticles was achieved via cross-linking of reactive quinones produced in the oxidation of DOPA by Ag(I) or Au(III) ions. Because the polymer used in this study has a branched architecture, cross-linking reactions promoted network formation. Although Ag nanoparticle formation within hydrogels may be influenced by higher reagent concentration (10× higher) and the presence of the polymer network, these data support our hypothesis of silver particle formation resulting from the redox reaction between silver ions and the catechol-containing polymer, and offer qualitative insight into the shape and size of the Ag nanoparticles embedded within the hydrogel. Silver release studies demonstrated a sustained release of silver over 2 weeks (Figure 7). The low concentrations of silver (1.3 μM, ~1.3 μg released/day in 5 mL of PBS) are not known to be cytotoxic to various mammalian cell lines, but are toxic to many bacterial cells.[18, 32] The results suggest that these gels have the potential to inhibit bacterial growth, while not significantly effecting mammalian cell viability.

To probe bacterial cell toxicity we used a traditional zone of inhibition assay to determine if the released silver was toxic to bacteria (Table 2). We found comparable bacterial growth inhibition around the Ag-cPEG gel disk when compared to a tetracycline positive control disk. Our negative control $NaIO_4$-cPEG showed no bacterial growth inhibition. Bacterial growth on thin cPEG hydrogel films was reduced by >99.9 % over 24 h, compared to TiO_2 control surfaces (Figure 8). Due to the low silver content and ultrathin nature of the Ag-cPEG coating (~25nm), this result is unlikely to reflect off-surface antibacterial effects correlated to Ag(I) release from the coating. Rather, it is considered to be a result of the high PEG content of the coating, which is a fouling resistant polymer. Mammalian cell viability did not appear to be significantly affected by the low concentrations of silver released (Figure 9). We surmise that the low degree mammalian cell attachment to hydrogel films (Figure 10) was not a result of toxic effects of Ag(I) release from the coating, as media conditioned by exposure to bulk Ag-cPEG hydrogels was not cytotoxic (Figure 9). Instead, these results simply reflect the antifouling nature of the PEG coating. Given these results, Ag-cPEG hydrogels materials appear to release silver at concentrations sufficient for an antibacterial effect without significantly altering mammalian cell viability.

5. Conclusions

Antibacterial hydrogels and coatings were synthesized by redox reactions between soluble Ag(I) and catechol functional groups of a branched PEG polymer. These gels can take the form of free-standing and in-situ forming bulk hydrogels or thin hydrogel coatings on solid substrates. Reduction of Ag(I) to Ag(0) was coupled with oxidative covalent polymerization of catechols to form polymer hydrogels containing entrapped Ag nanoparticles. Thus, the role of silver is to induce spontaneous polymer gelation as well as instill intrinsic antibacterial properties into the hydrogel. Mammalian cell toxicity was not observable under the conditions of our experiments, suggesting that the antibacterial properties fall within the therapeutic window of silver concentrations, i.e., they are sufficient to kill bacterial cells without significantly affecting mammalian cell viability. In coating form, the hydrogels were resistant to both mammalian and bacterial cell attachment. In the future it may be possible to exploit Ag-cPEG hydrogels as tissue adhesives or sealants, since the adhesive properties of catechols found in native mussel adhesive proteins and synthetic polymers are well documented. In some surgical situations it may be advantageous for an adhesive hydrogel to be inherently antibacterial, for example in the case of external wound repair, surgery of the

gastrointestinal tract, or even as a prophylactic measure in general surgical procedures involving adhesives and sealants. Ag-cPEG coatings may be useful for reducing bacterial colonization and biofilm formation on a variety of medical and nonmedical devices. While further work will be needed to evaluate the efficacy of Ag-cPEG hydrogels for these applications, we believe these hydrogels have the potential to reduce infection rates in applications where tissue sealants are needed or where biomaterial coatings could be employed.

Supplementary Material

Refer to Web version on PubMed Central for supplementary material.

Acknowledgments

The authors would like to acknowledge Brian Jao for his assistance with the MTS assays and Devin Barrett for helpful suggestions in the preparation of this manuscript. DEF was supported by NIH NRSA F30 HL096292. JGR was supported by NIH EB005772-02S1. This research was supported by NIH grants DE014193 and EB005772. The following Northwestern Univ. facilities were used for data collection: IMSERC (NMR and MS), KECK Biophysics (UV-Vis, GPC), QBIC (ICP-MS) and NUANCE (TEM).

References

1. Lee BP, Messersmith PB, Israelachvili JN, Waite JH. Mussel-inspired adhesives and coatings. Annu Rev Mater Res. 2011; 41:99–132. [PubMed: 22058660]
2. Brubaker CE, Kissler H, Wang L-J, Kaufman DB, Messersmith PB. Biological performance of mussel-inspired adhesive in extrahepatic islet transplantation. Biomaterials. 2010; 31:420–427. [PubMed: 19811819]
3. Lee BP, Dalsin JL, Messersmith PB. Synthesis and gelation of DOPA-modified poly(ethylene glycol) hydrogels. Biomacromolecules. 2002; 3:1038–1047. [PubMed: 12217051]
4. Deming TJ. Mussel byssus and biomolecular materials. Curr Opin Chem Biol. 1999; 3:100–105. [PubMed: 10021411]
5. Waite JH. Natures underwater adhesive specialist. Int J Adhes Adhes. 1987; 7:9–14.
6. Waite JH, Tanzer ML. Polyphenolic substance of *Mytilus edulis*: novel adhesive containing L-DOPA and hydroxyproline. Science. 1981; 212:1038–1040. [PubMed: 17779975]
7. Yu M, Hwang J, Deming TJ. Role of L-3,4-dihydroxyphenylalanine in mussel adhesive proteins. J Am Chem Soc. 1999; 121:5825–5826.
8. Yu M, Deming TJ. Synthetic polypeptide mimics of marine adhesives. Macromolecules. 1998; 31:4739–4745. [PubMed: 9680407]
9. Westwood G, Horton TN, Wilker JJ. Simplified polymer mimics of cross-linking adhesive proteins. Macromolecules. 2007; 40:3960–3964.
10. Shao H, Bachus KN, Stewart RJ. A water-borne adhesive modeled after the sandcastle glue of *P. californica*. Macromol Biosci. 2009; 9:464–471. [PubMed: 19040222]
11. Brubaker CE, Messersmith PB. Enzymatically degradable mussel-inspired adhesive hydrogel. Biomacromolecules. 2011; 12:4326–4334. [PubMed: 22059927]
12. Peppas NA, Hilt JZ, Khademhosseini A, Langer R. Hydrogels in biology and medicine: from molecular principles to bionanotechnology. Adv Mater. 2006; 18:1345–1360.
13. Peppas NA, Huang Y, Torres-Lugo M, Ward JH, Zhang J. Physicochemical foundations and structural design of hydrogels in medicine and biology. Annu Rev Biomed Eng. 2000; 2:9–29. [PubMed: 11701505]
14. Klasen HJ. Historical review of the use of silver in the treatment of burns. I. early uses. Burns. 2000; 26:117–130. [PubMed: 10716354]
15. Klasen HJ. A historical review of the use of silver in the treatment of burns. II. renewed interest for silver. Burns. 2000; 26:131–138. [PubMed: 10716355]

16. Leaper DJ. Silver dressings: their role in wound management. Int Wound J. 2006; 3:282–294. [PubMed: 17199764]
17. Vermeulen H, van Hattem JM, Storm-Versloot MN, Ubbink DT, Westerbos SJ. Topical silver for treating infected wounds. Cochrane Database Syst Rev. 2007 Available from URL: http://www.mrw.interscience.wiley.com/cochrane/clsysrev/articles/CD005486/frame.html.
18. Russell, AD.; Hugo, WB. Antimicrobial activity and action of silver. In: Ellis, GP.; Luscombe, DK., editors. Progress in Medicinal Chemistry. Amsterdam: Elsevier; 1994. p. 351-370.
19. Storm-Versloot MN, Vos CG, Ubbink DT, Vermeulen H. Topical silver for preventing wound infection. Cochrane Database Syst Rev. 2010 Available from URL: http://www.mrw.interscience.wiley.com/cochrane/clsysrev/articles/CD006478/frame.html.
20. Goldmann DA, Weinstein RA, Wenzel RP, Tablan OC, Duma RJ, Gaynes RP, et al. Strategies to prevent and control the emergence and spread of antimicrobial-resistant microorganisms in hospitals. JAMA. 1996; 275:234–240. [PubMed: 8604178]
21. Alt V, Bechert T, Steinrücke P, Wagener M, Seidel P, Dingeldein E, et al. An in vitro assessment of the antibacterial properties and cytotoxicity of nanoparticulate silver bone cement. Biomaterials. 2004; 25:4383–4391. [PubMed: 15046929]
22. Wright JB, Lam K, Buret AG, Olson ME, Burrell RE. Early healing events in a porcine model of contaminated wounds: effects of nanocrystalline silver on matrix metalloproteinases, cell apoptosis, and healing. Wound Repair Regen. 2002; 10:141–151. [PubMed: 12100375]
23. Schumm K, Lam TBL. Types of urethral catheters for management of short-term voiding problems in hospitalised adults. Cochrane Database Syst Rev. 2008 Available from URL: http://www.mrw.interscience.wiley.com/cochrane/clsysrev/articles/CD004013/frame.html.
24. Varaprasad K, Mohan YM, Ravindra S, Reddy NN, Vimala K, Monika K, et al. Hydrogel–silver nanoparticle composites: a new generation of antimicrobials. J Appl Polym Sci. 2010; 115:1199–1207.
25. Zan X, Kozlov M, McCarthy TJ, Su Z. Covalently attached, silver-doped poly(vinyl alcohol) hydrogel films on poly(L-lactic acid). Biomacromolecules. 2010; 11:1082–1088. [PubMed: 20307097]
26. Murali Mohan Y, Vimala K, Thomas V, Varaprasad K, Sreedhar B, Bajpai SK, et al. Controlling of silver nanoparticles structure by hydrogel networks. J Colloid Interface Sci. 2010; 342:73–82. [PubMed: 19883919]
27. Black KCL, Liu Z, Messersmith PB. Catechol redox induced formation of metal core-polymer shell nanoparticles. Chem Mater. 2011; 23:1130–1135. [PubMed: 21666825]
28. Hackman RH, Todd AR. Some observations on the reaction of catechol derivatives with amines and amino acids in presence of oxidizing agents. Biochem J. 1953; 55:631–637. [PubMed: 13115345]
29. Baudisch O, Dyer E. The o-quinone test for cysteine. J Biol Chem. 1933; 99:485–492.
30. He L, Fullenkamp DE, Rivera JG, Messersmith PB. pH responsive self-healing hydrogels formed by boronate-catechol complexation. Chem Commun. 2011; 47:7497–7499.
31. Waite JH. Calculating extinction coefficients for enzymatically produced o-quinones. Anal Biochem. 1976; 75:211–218. [PubMed: 822748]
32. Travan A, Pelillo C, Donati I, Marsich E, Benincasa M, Scarpa T, et al. Non-cytotoxic silver nanoparticle-polysaccharide nanocomposites with antimicrobial activity. Biomacromolecules. 2009; 10:1429–1435. [PubMed: 19405545]

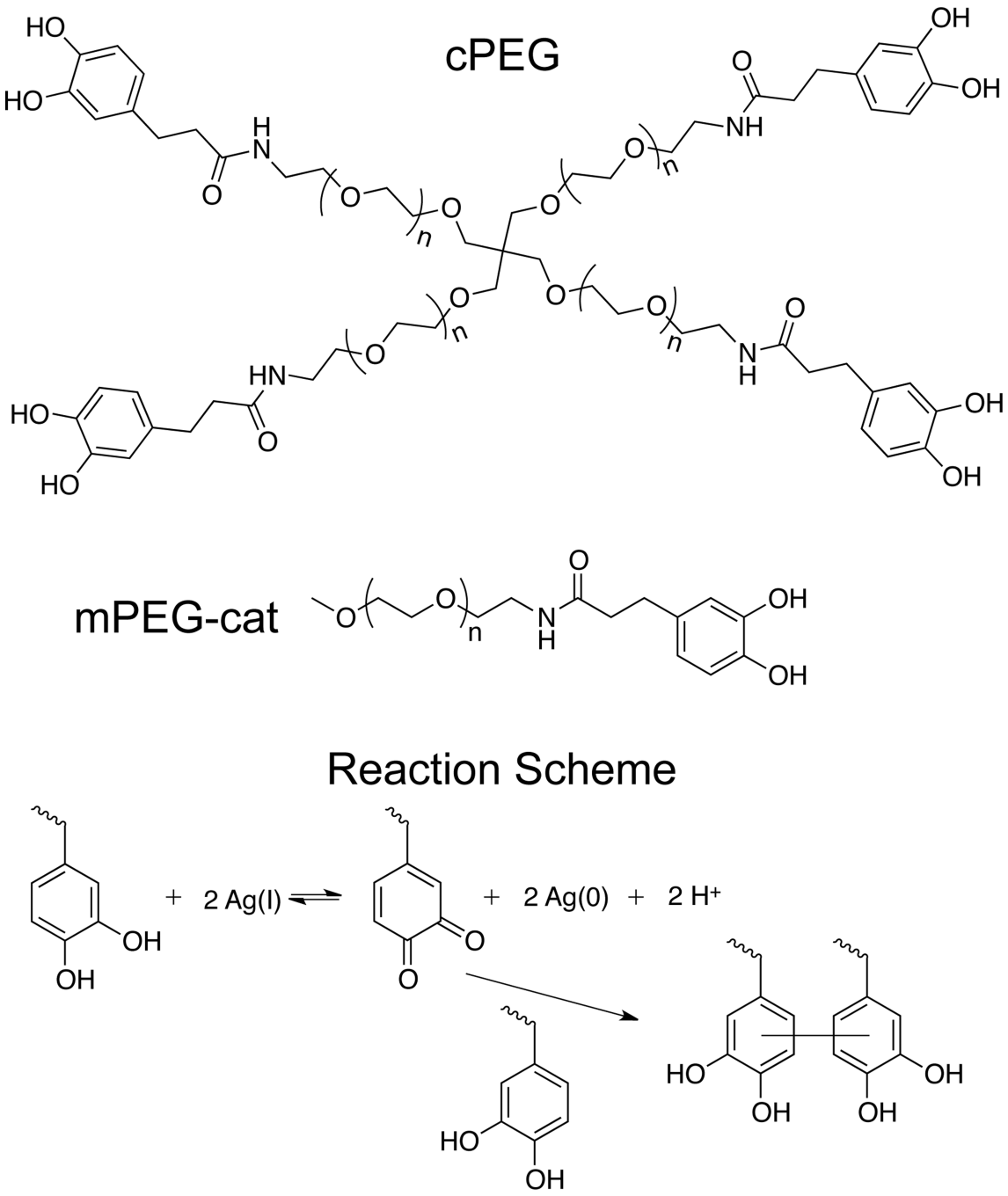

Figure 1.
Molecules synthesized and proposed reaction scheme. cPEG was used to form hydrogels and mPEG-Cat was used for model GPC studies of the reaction. Catechol reduction of Ag(I) allows for quinone-initiated radical coupling to catechols as well as simultaneous silver nanoparticle formation.

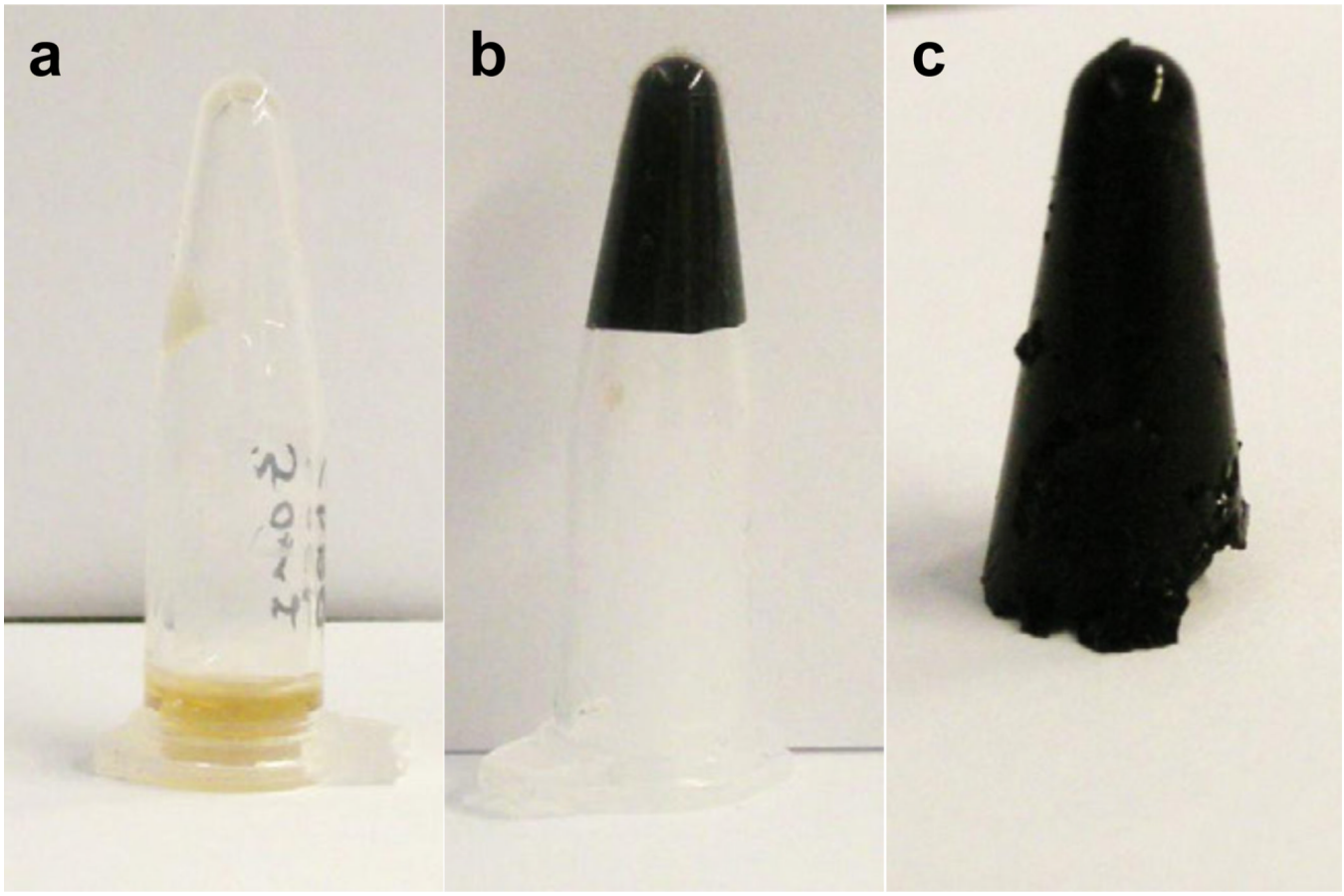

Figure 2.
Images of: (a) cPEG solution in Tris buffer before $AgNO_3$ addition. (b) Ag-cPEG hydrogel formed after the addition of $AgNO_3$. (c) Free standing Ag-cPEG hydrogel after removal from vial in (same gel as in b, Ag: catechol mol ratio = 2.0).

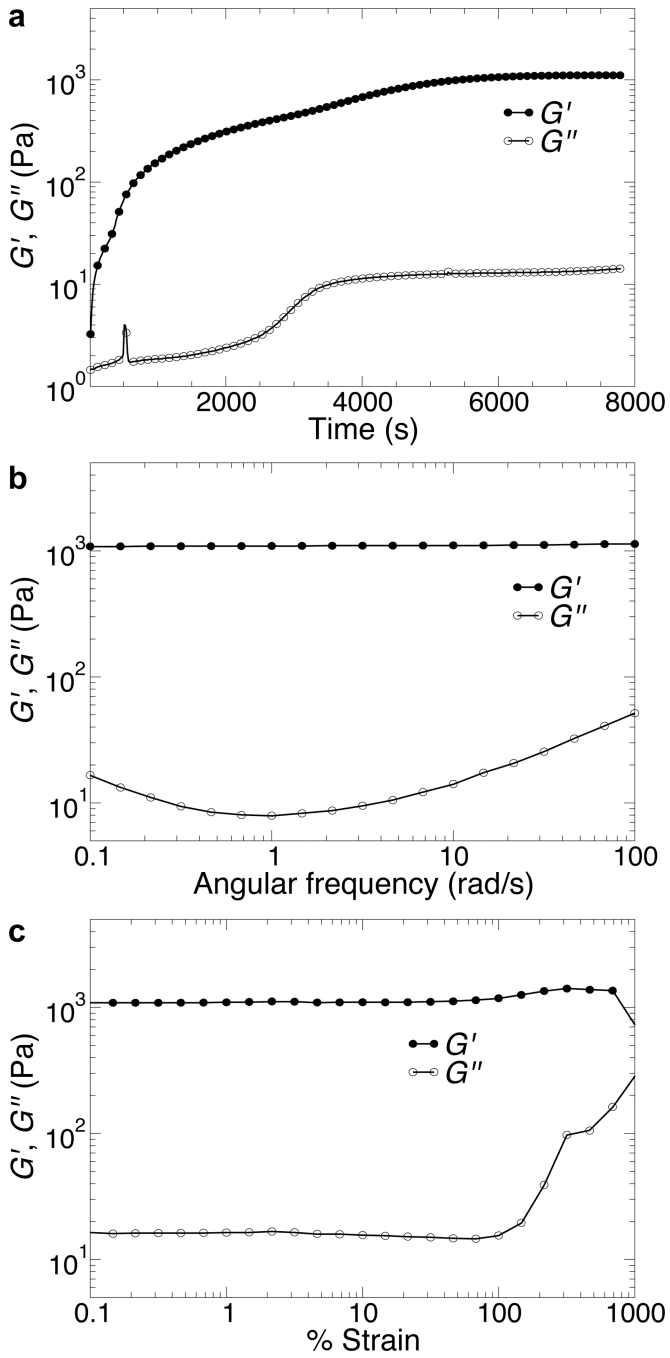

Figure 3.
Rheological characterization of cPEG-Ag hydrogel formation: (a) Dynamic storage (G') and loss (G'') moduli as a function of time after addition of $AgNO_3$ (Ag:catechol = 2.0). (b) Frequency sweep performed at 5 % strain. (c) Strain sweep performed at 10 rad/s.

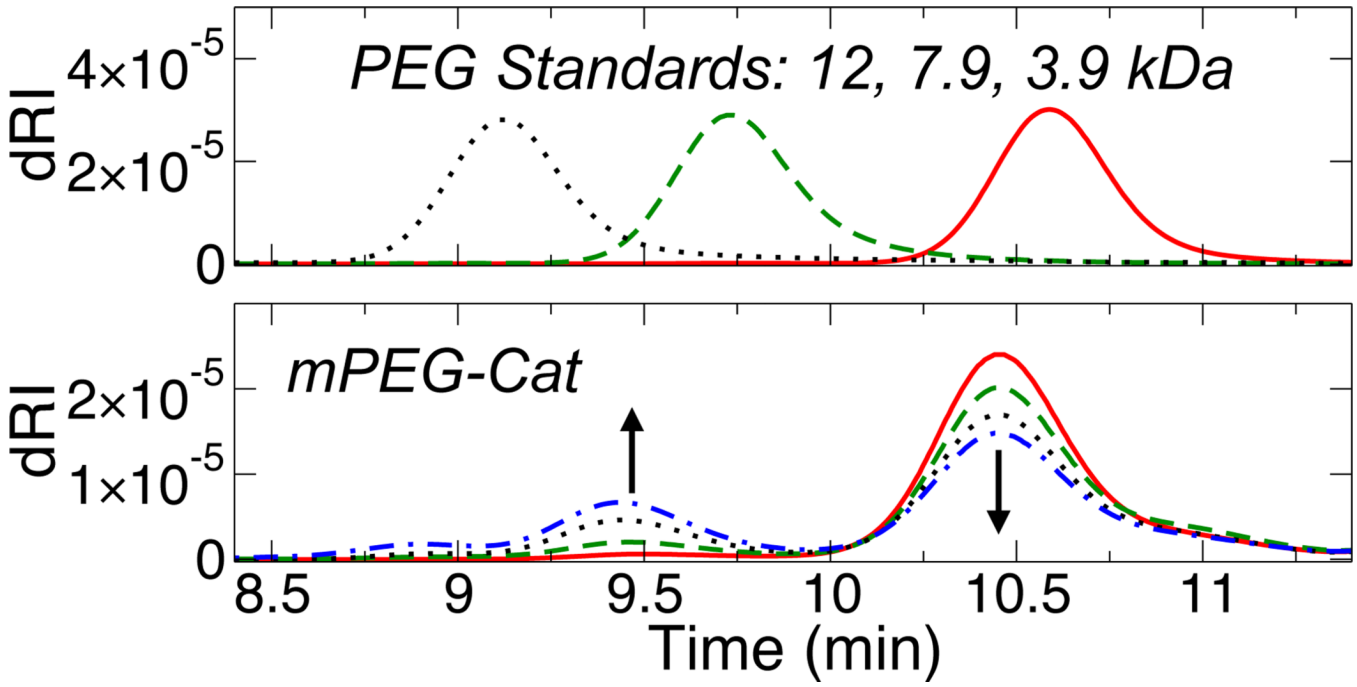

Figure 4.

Model GPC study of gel formation conditions using the monofucntional polymer mPEG-Cat. Top: PEG standards. Bottom: mPEG-Cat reaction with 0×, 1×, 2×, and 4× Ag(I) relative to catechol endgroup at 60 mM catechol concentration. Arrows point in the direction of increasing Ag(I) concentration. Monomer peak (~10–11 min) decreases, while multimer (~8.5–10 min) increases with increased Ag(I) concentrations.

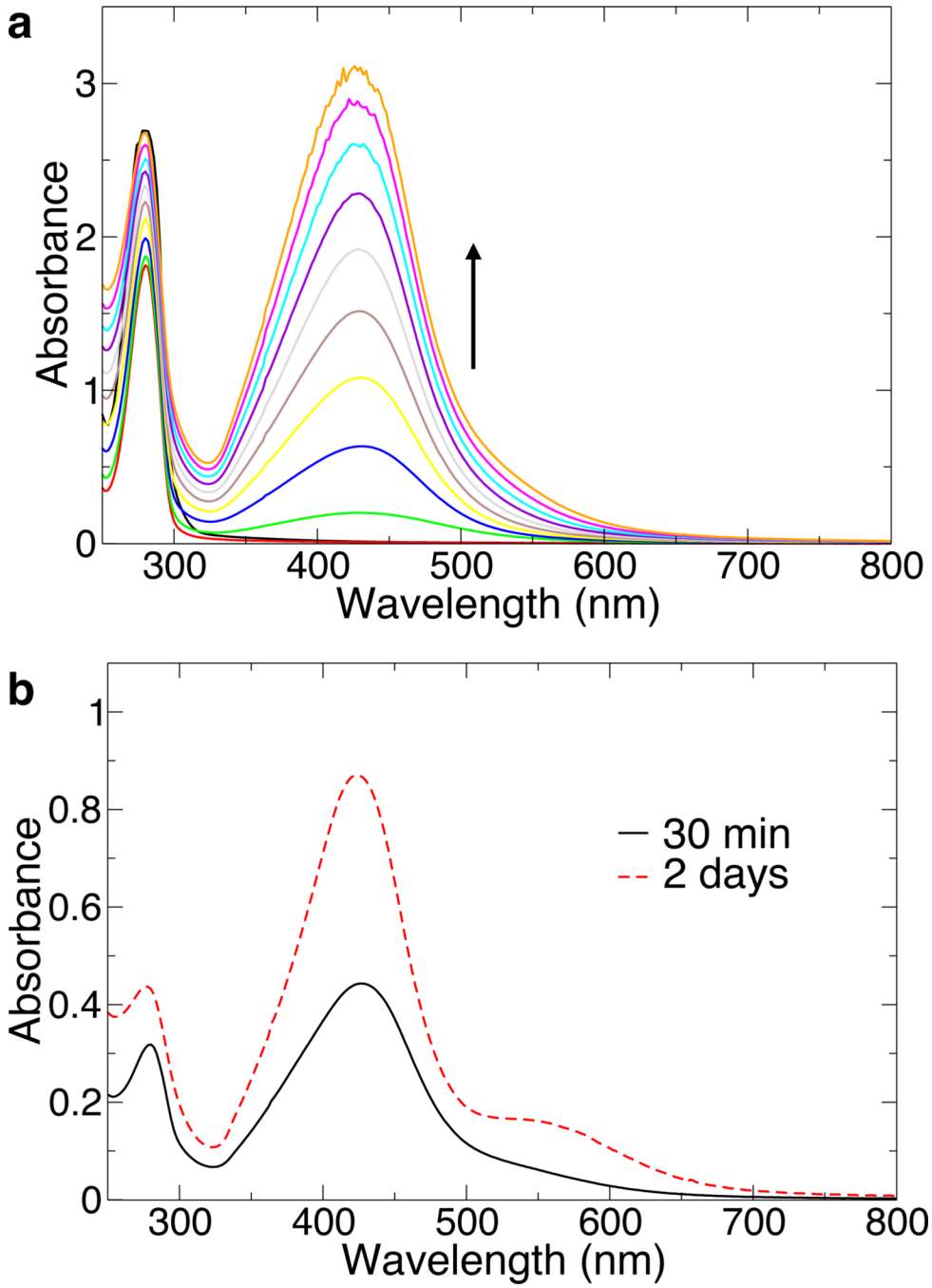

Figure 5.
UV-Vis characterization of silver nanoparticle formation. (a) Time-dependent UV-Vis spectroscopy of 100× dilution of Ag-cPEG gel reaction at 2:1 Ag:catechol ratio. The spectra shown correspond to reaction times of 0–27 min, with the arrow indicating the growth of Ag plasmon band with time. (b) 10× dilution of sample from (a) after 30 min and 2 days of reaction.

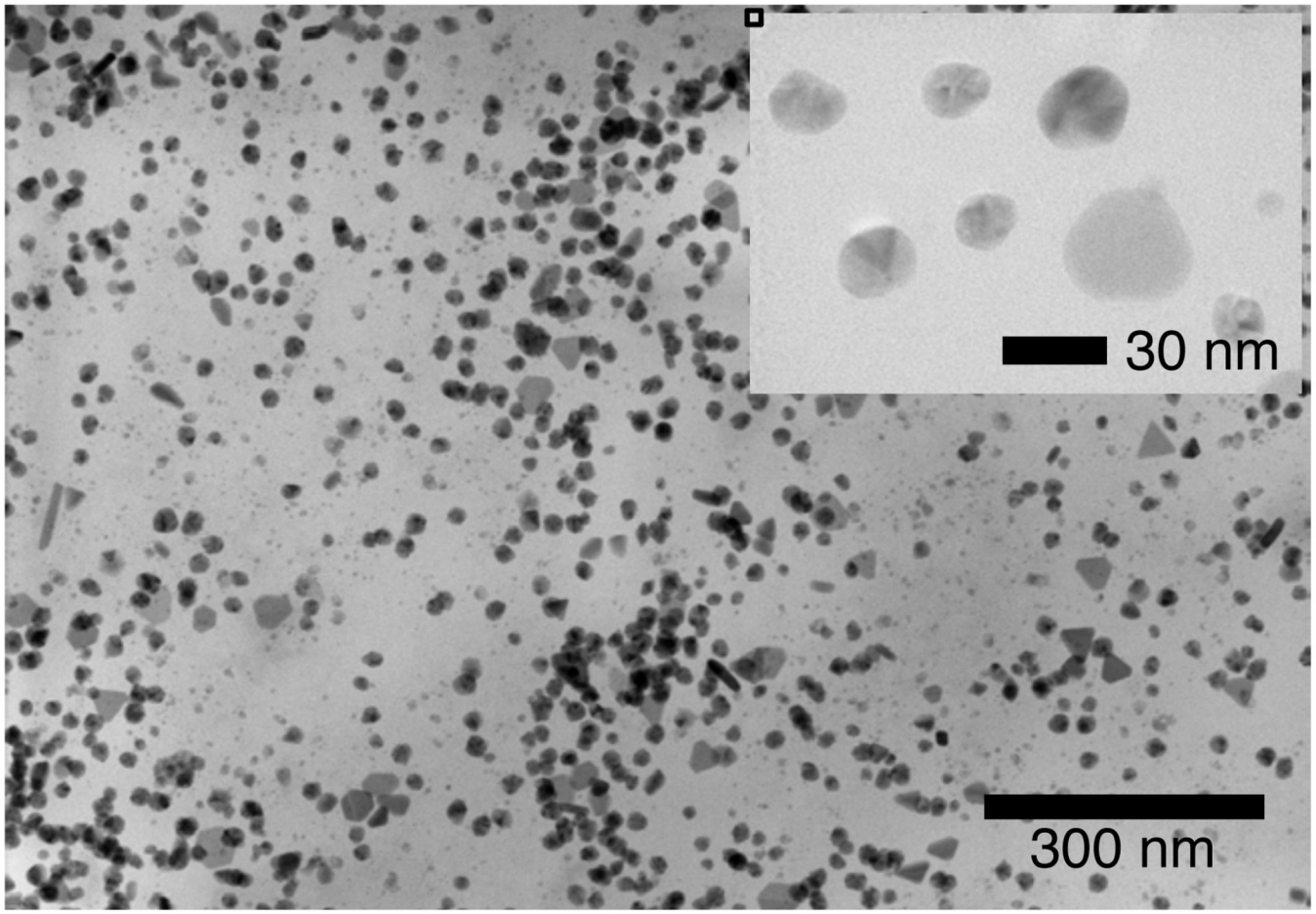

Figure 6.
TEM images of silver nanoparticles formed by reaction of Ag(I) with cPEG (2:1 Ag(I):catechol). Inset shows higher magnification image of same nanoparticles.

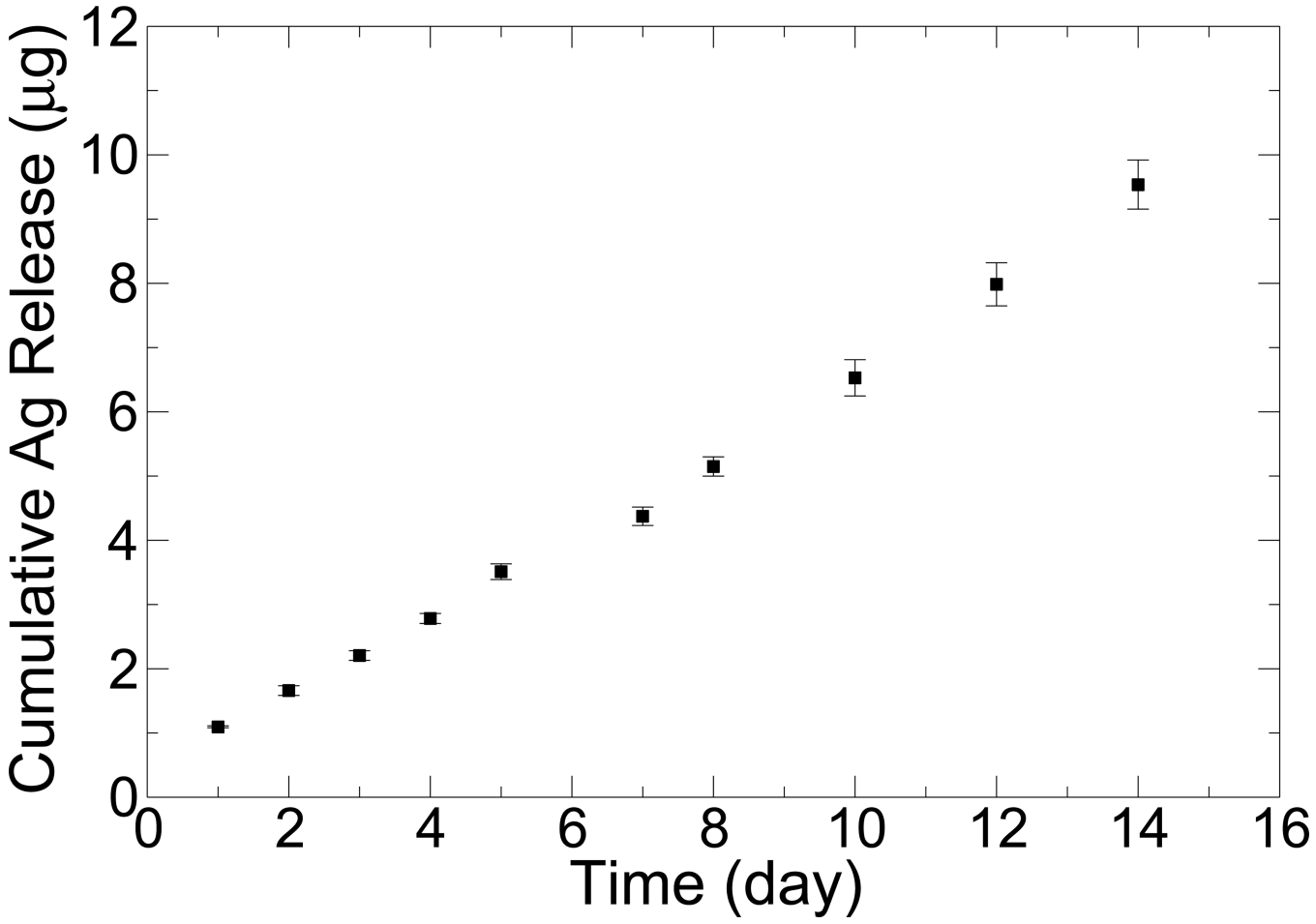

Figure 7.
Cumulative silver release from Ag-cPEG hydrogels as a function of time.

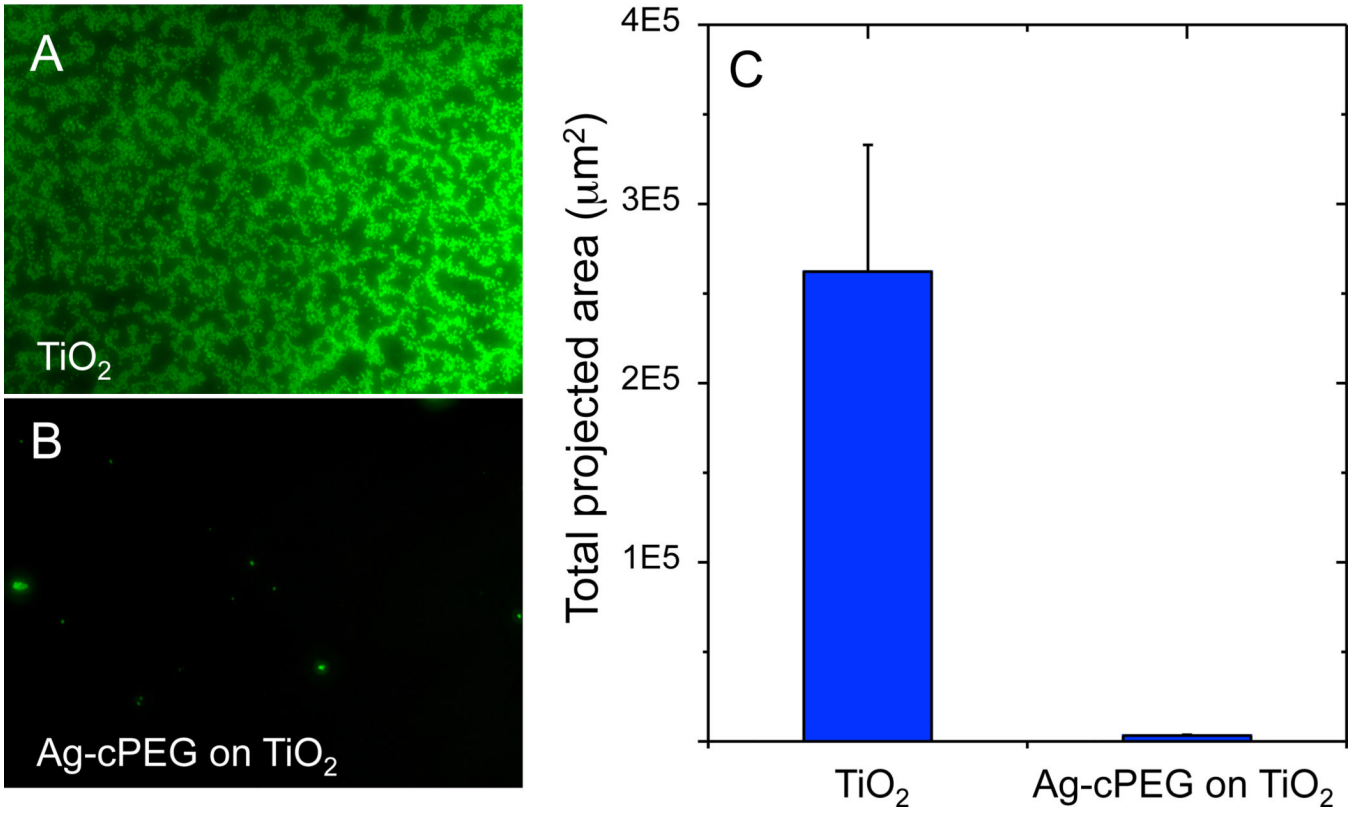

Figure 8.
Bacterial attachment onto Ag-cPEG coatings. (A) Representative fluorescence microscopy images (40×) of uncoated (top) and Ag-cPEG coated (bottom) TiO_2 exposed to *S. epidermidis* for 24 h. (B) Quantitative *S. epidermidis* cell attachment data obtained from image analysis.

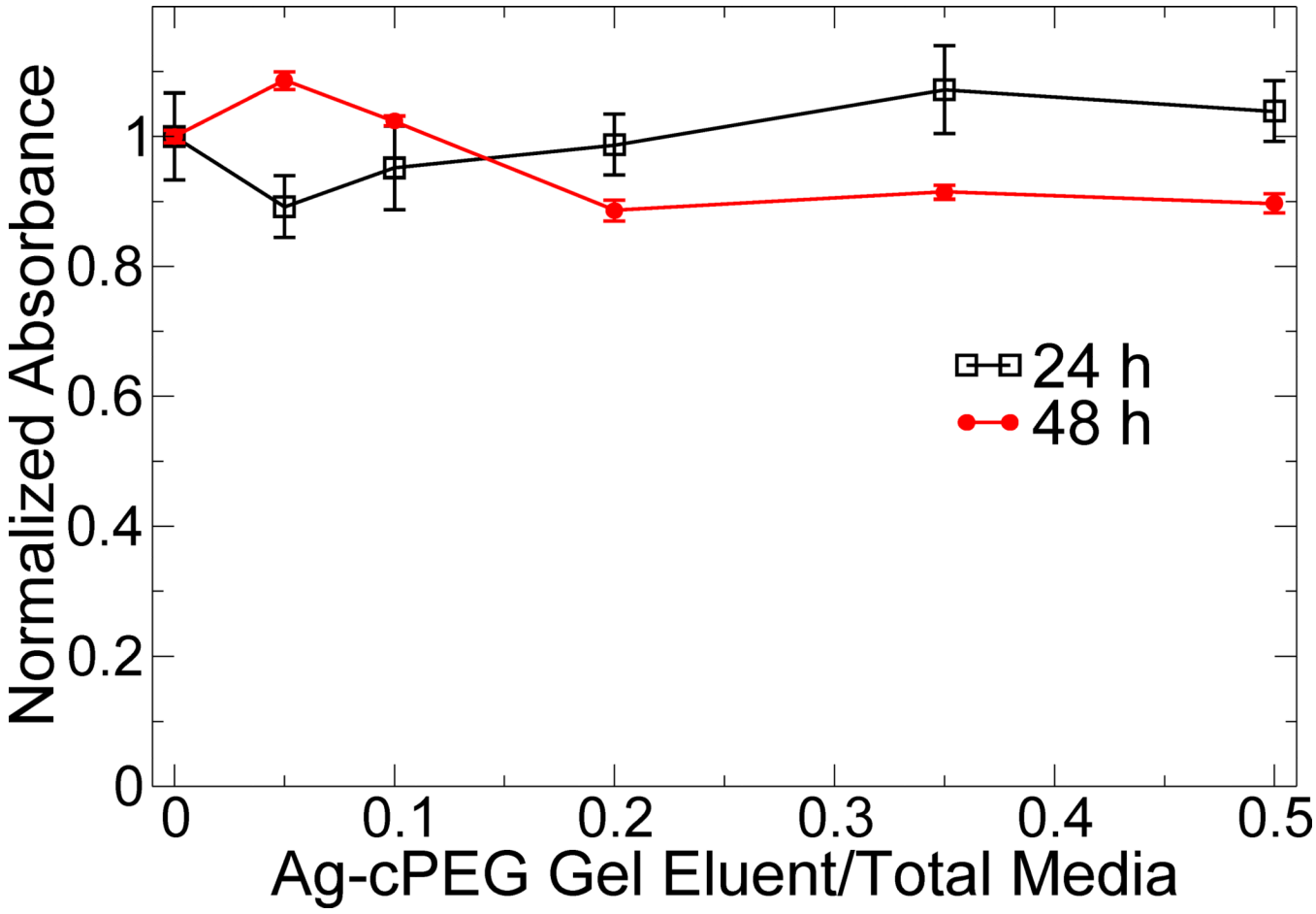

Figure 9.
Mammalian cell viability assessment. MTS assay was used to determine the effect of the eluent from Ag-cPEG gels on 3T3 fibroblasts. At 24 and 48 h time points, cells appear viable at all ratios of Ag-cPEG eluent/total media. Error bars represent the standard deviation of 3 samples.

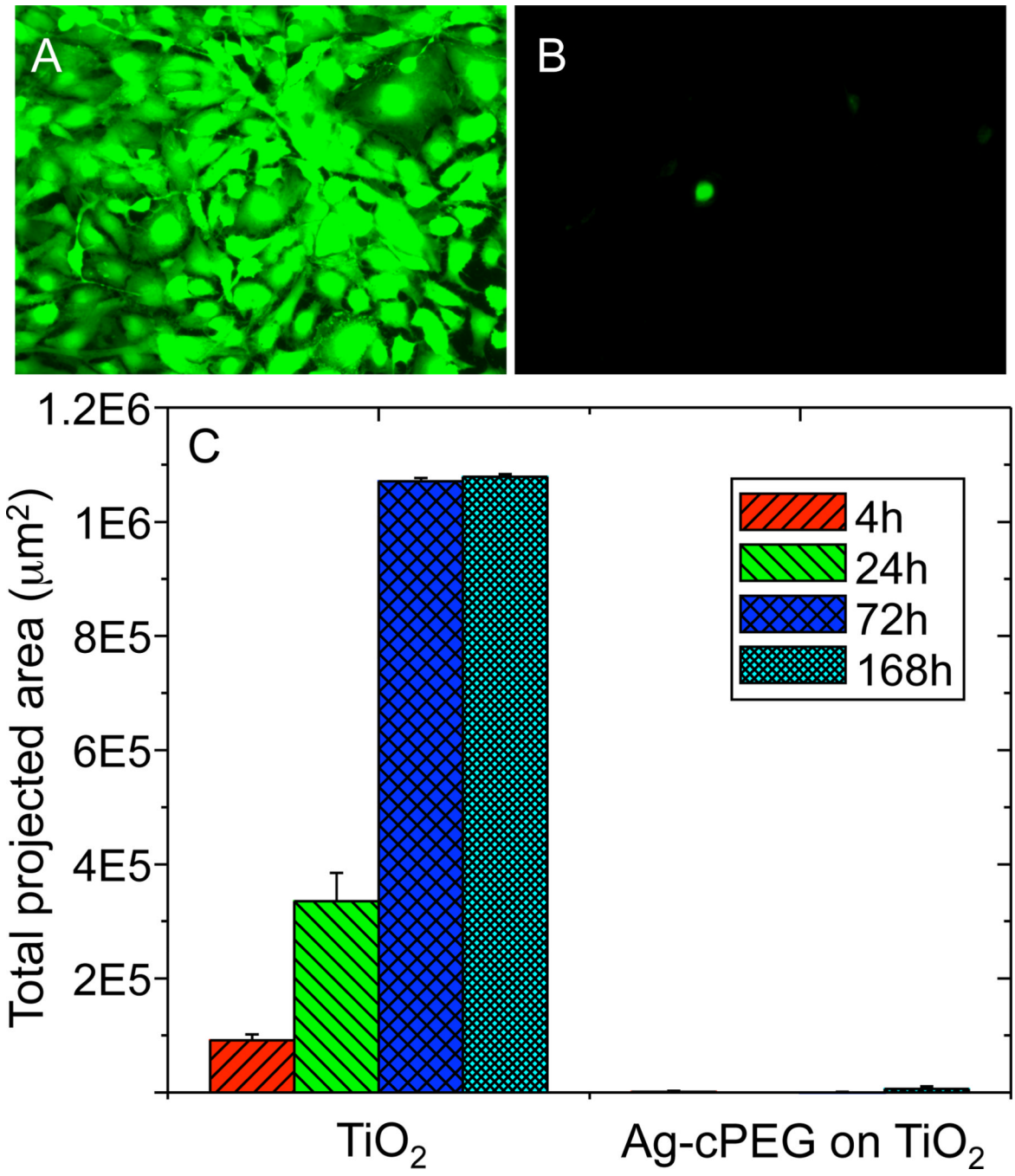

Figure 10.

Mammalian cell attachment onto Ag-cPEG coatings. (A) Representative fluorescence microscopy images (40×) of uncoated (top) and Ag-cPEG coated (bottom) TiO_2 after exposure to 3T3 cells for 72 h. Cells were stained with MTS. (B) Quantitative 3T3 cell attachment data obtained from image analysis of substrates exposed to cells for up to 7 d.

Table 1

Effect of Ag:catechol stoichiometry on Ag-cPEG hydrogel gelation time and swelling.

Mol Ratio of $[Ag^+]$:[Catechol]	Gelation Time	Gel swelling in PBS after 7 days
0:1	no gel formed	-
0.5:1	60 min	gel dissolved
1:1	40 min	gel dissolved
2:1	20 min	325% +/− 25%
4:1	10 min	225% +/− 21%

Table 2

Antibacterial activity of Ag-cPEG hydrogels.

Sample tested	**Original disk diameter (mm)**	**Zone of inhibition (mm) (*S. epidermidis*)**	**Zone of inhibition (mm) (*P. aeruginosa*)**
$NaIO_4$-cPEG (control) gel disk	11.8	n/a	n/a
Ag-cPEG gel disk	11.8	17.2 +/− 0.5	18.4 +/− 0.7
Tetracycline disk	7.2	11.4 +/− 0.3	12.2 +/− 0.2